

Computational study on the geometry optimization and excited – State properties of Riboflavin by ArgusLab 4.0.1

Ambreen Hafeez*, Afshan Naz, Sadaf Naeem, Khalida Bano and Naheed Akhtar

Department of Biochemistry, Biophysics Research Unit, University of Karachi, Pakistan

Abstract: Riboflavin (vitamin B₂) belongs to a group of respiratory enzymes that occur widely in animals and plants participating in vital oxidation- reduction processes in the body. A computational study was conducted on riboflavin by ArgusLab 4.0.1 to obtain the most active conformation of riboflavin and to analyze its excited-state properties. The best conformation of riboflavin was found to be -199.2173 kcal/mol which is the minimum potential energy calculated by geometry convergence function by ArgusLab software; performed according to Hartree-Fock calculation method. Electronic transition states (ground and excited), were also calculated and visualized by semi-empirical ZINDO method by ArgusLab from which molecular properties such as energies, wave function and dipole moments were established. All the results obtained from geometry optimization and excited-state properties lead us to delineate the active sites with charged groups of riboflavin to interact with the receptors. Such types of investigations are significant for drug -receptor interactions.

Keywords: ArgusLab 4.0.1, geometry optimization, excited states, potential energy, Riboflavin

INTRODUCTION

Riboflavin (vitamin B₂) belongs to the flavin group of compounds which constitute the yellow chromophoric and redox-active prosthetic group of a class of respiratory enzymes occurring widely in animals and plants, namely the flavoproteins. It is the precursor in the biosynthesis of the coenzymes FMN (flavinmononucleotide) and FAD (flavinadeninedinucleotide). Flavins are the class of compounds which are broadly investigated in terms of their biological functions (Miura, 2001), photosensitivity (Penzer and Radda, 1970) and nutritional aspects (Powers, 2003). They are also involved in *photosensitized* degradation of a number of compounds such as amines (Encinas *et al.*, 2002), retinoid (Fu *et al.*, 2003), cyanocobalamin (Ahmad *et al.*, 1992), DNA (Dahl and Richardson, 1980), RNA (Burgstaller *et al.*, 1997) etc.

Though the above mentioned studies have been carried out on riboflavin, but no computational studies have been made so far on conformational analysis (geometry optimization) and excited-state properties of riboflavin by modern quantum chemical methods. The geometry of a molecule has a great impact on its energy level and physical and chemical properties. As the molecule rotates, it adopts different conformations and spatial arrangements to achieve one of the stable states of *lowest energy* (Crowder, 1986). The total molecular energy can be evaluated in terms of potential energy surface as a sum of energies associated with each type of bonded interactions i.e. bond length, bond angle and dihedral angle as well as non-bonded interactions (van der Waals and electrostatic) taking place in a molecule and on atomic properties of a molecule (Cramer, 2004).

In molecular mechanics, potential energy is calculated using force field where the atoms move without breaking of bonds until the energy of the molecule reaches to a minimum also referred as *energy minimization*. These minimum energy structures are equilibrium structures representing minima on the potential energy surface (Hirst, 1990).

As far as vitamins are concerned, several studies have been done on the conformational analysis of vitamins specially vitamin D and K by different computational techniques (Makin and Jones, 2010; Sachiko *et al.*, 1999; Sanchez *et al.*, 2009).

Electronic excitations resulting from energy absorption in the UV/visible region usually involves changes in the electronic state of a molecule leading to the promotion of electron in either π bonding or non bonding orbital in ground-state (S_0) to the π^* antibonding orbital (i.e. $\pi \rightarrow \pi^*$ or $n \rightarrow \pi^*$ transitions respectively) in excited states (S_1) (Mortimer, 2000). The absorption spectrum of typical flavins such as riboflavin in aqueous solution consist of four maxima at 450, 370, 265 and 223 nm having high molar absorptivities indicative of $\pi \rightarrow \pi^*$ ($S_0 \rightarrow S_1$) electronic transitions. Flavins exhibit a characteristic fluorescence (λ_{\max} 520 nm) due to $S_1 \rightarrow S_0$ transition in aqueous solution, at pH 7 (Weber and Teal, 1957). In solvents less polar than water, the fluorescence maximum is usually shifted to shorter wavelengths (Visser and Muller, 1979).

The present work describes the computer aided geometry optimization (active conformation) and calculation of excited state properties of riboflavin (Vit B₂) by ArgusLab 4.0.1 software (Thompson, 2004).

*Corresponding author e-mail: ambreenfv@hotmail.com

ArgusLab is molecular modeling software and the latest version 4.0.1 is capable of performing various molecular calculations such as geometry optimization, molecular structure visualization, determination of vibrational frequencies of functional groups etc to provide users with molecular building analyses (Oda and Takahashi, 2009).

MATERIALS AND METHODS

The structure of riboflavin (Merck) was drawn and constructed using window based program of ArgusLab and ACD Lab Chem Sketch software. Conformational analysis (geometry optimization) of riboflavin was carried out using PM3 semi-empirical QM parameterization (Stewart, 1989) according to Hartree-Fock calculation method by ArgusLab 4.0.1 software. Geometry of the molecule was converged after the molecule is drawn and cleaned in ArgusLab and the program then computes the energy until the maximum cycles reached for the convergence (stopping point) of the molecule. Grid data was produced to generate surfaces which is a cubic grid of points around the molecule where various properties can be calculated such as electron densities, electrostatic potentials for any state i.e. ground state =0 to excited-states 1, 2, 3 etc. and any of the orbital. ArgusLab subsequently uses these grid files to display surfaces for the relevant properties. Many of these kinds of surfaces are shown and described in this work.

The electronic excited-state calculations were carried out by ZINDO semi-empirical method (Ridley and Zerner, 1973; Zerner, 1991) which is parameterized for low-energy excited-states of organic and organo-metallic molecules. Electronic excitation spectrum of riboflavin was calculated by self consistent reaction field (SCRF) solvent model of Zerner and coworkers (Karelson and Zerner, 1992) and water was taken as a solvent.

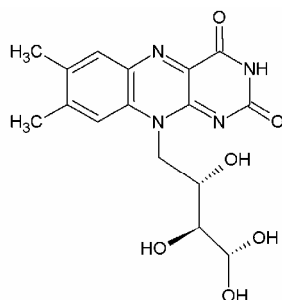
RESULTS

Fig. 1 shows the perspective view of riboflavin generated by ACD Lab Chem-sketch. Active conformation of riboflavin with labeled atoms is illustrated in fig. 2 by Argus Lab software. Fig. 3 shows the electron density clouds of riboflavin by ACD Labs 3D viewer software.

The decreasing potential energy is shown in fig. 4 through the geometry convergence map of the riboflavin as a function of changing rotation angles.

Atomic coordinates are given in table 1. Tables 2 and 3 represent the bond angles and bond lengths respectively calculated from geometry optimization of riboflavin.

Fig. 5 illustrates the frontier molecular orbitals i.e. Highest energy occupied molecular orbital (HOMO) and the lowest unoccupied (LUMO) molecular orbital. Figs. 6,



7,8-dimethyl-10-[(2S,3S)-2,3,4,4-tetrahydroxybutyl]benzo[g]pteridine-2,4(3H,10H)-dione

Molecular Formula	= C ₁₈ H ₁₈ N ₄ O ₆
Formula Weight	= 362.33732
Composition	= C(53.04%) H(5.01%) N(15.46%) O(26.49%)
Molar Refractivity	= 86.49 ± 0.5 cm ³
Molar Volume	= 211.4 ± 7.0 cm ³
Parachor	= 620.1 ± 8.0 cm ³
Index of Refraction	= 1.754 ± 0.05
Surface Tension	= 73.9 ± 7.0 dyne/cm
Density	= 1.71 ± 0.1 g/cm ³
Dielectric Constant	= Not available
Polarizability	= 34.28 ± 0.5 10 ⁻²⁴ cm ³
Monoisotopic Mass	= 362.122634 Da
Nominal Mass	= 362 Da
Average Mass	= 362.3373 Da
M+	= 362.122086 Da
M-	= 362.123183 Da
[M+H] ⁺	= 363.129911 Da
[M+H] ⁻	= 363.131008 Da
[M-H] ⁺	= 361.114261 Da
[M-H] ⁻	= 361.115358 Da

Fig. 1: Perspective view of Riboflavin

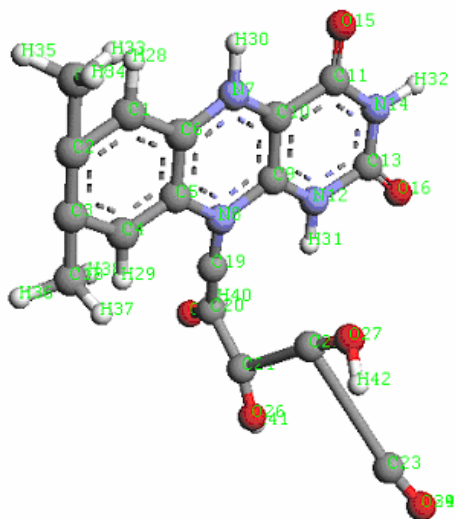


Fig. 2: Active conformation of Riboflavin with optimized geometry.

7 and 8 represent the ESP mapped electron density surface, electron density difference and ESP difference of riboflavin respectively.

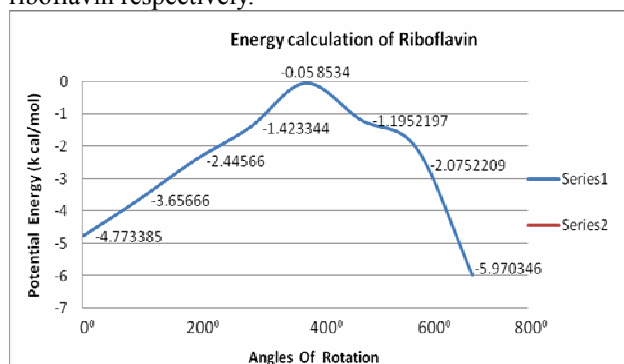


Fig. 4: Potential Energy Geometry Convergence Map of Riboflavin.

DISCUSSION

The active conformation and electron density clouds of riboflavin represent the arrangement of electrons around the atom which determines the energy level of riboflavin. The geometry convergence map of riboflavin clearly shows a decrease in potential energy with the progress of rotation. Among the molecular orbitals, HOMO is a non bonding type while the LUMO is a π molecular orbital. The positive and negative charges are indicated by blue and red color, respectively. LUMO map can provide an idea for nucleophilicity. ArgusLab can also map the electronic properties onto the surface of electron density. Fig.6a shows the Electrostatic Potential (ESP) of riboflavin ground state mapped onto the electron density surface for the ground state rendered as mesh to reveal the underlying structure. Fig. 6b exhibits the complete surface. The colors are the values of the ESP energy (in

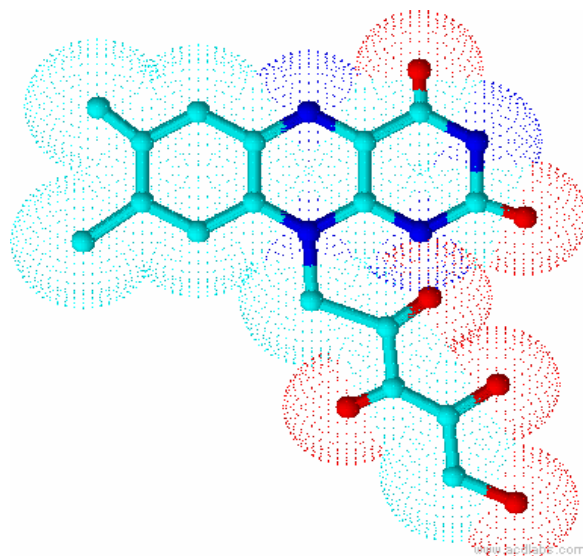


Fig. 3: Electron density clouds of Riboflavin by ACD Labs 3D viewer.

Hartrees) at the points on the electron density surface. The red color indicates the enhanced electron density around the oxygen-ends of the molecule representing the most negative regions of the ESP (region of highest stability) for a positive test charge where it would have favorable interaction energy. On the other hand the hydrogen-ends of the molecule, seen in magenta/blue color, shows the region of least stability for the positive test charge indicating the unfavorable interaction energy.

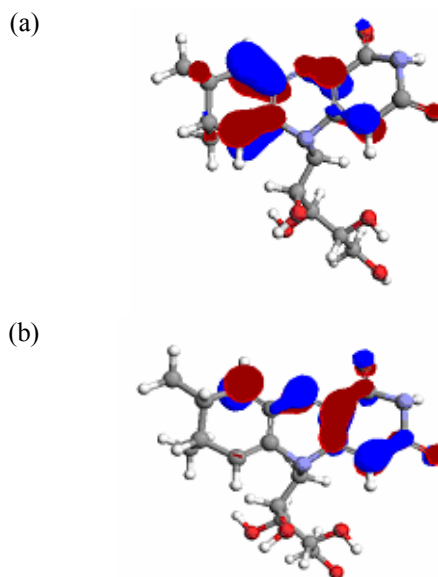


Fig. 5: Visualize the Frontier Molecular Orbitals (a) HOMO and (b) LUMO.

Thus an ESP-mapped density surface can be used to show the regions of a molecule that might be more favourable to *nucleophilic* or *electrophilic* attack, making these types of surfaces useful for the qualitative interpretations fig. 7

shows the difference of the excited state minus the ground state electron density for riboflavin. The $n \rightarrow \pi^*$ transition shows a positive electron density difference (blue regions) on the carbon atoms of the ribityl side chain while a negative electron density difference (red region) is seen around the keto and amino groups of riboflavin. Such a transition is dominated by the excitations from highest occupied to lowest unoccupied molecular orbital.

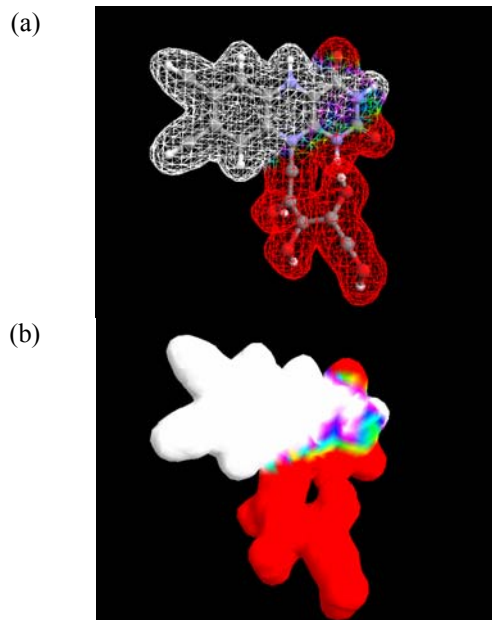


Fig. 6: Electrostatic potential (ESP) mapped electron density surface (a) mesh (b) opaque.

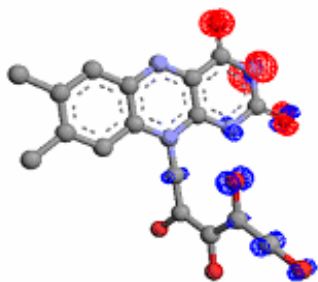


Fig. 7: Visualize the electron density difference of riboflavin (mesh).

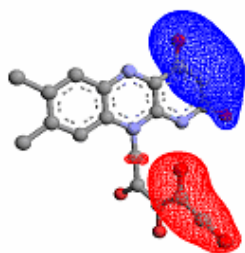


Fig. 8: ESP difference surface of riboflavin.

Fig. 8 shows how the ESP has changed by the movements of electrons in the excitation. The difference in the ESP

surface for $\pi \rightarrow \pi^*$ excited state minus the ground state clearly indicates the shift of electron density from the carbon atoms to the pteridine ring of the riboflavin dominating over the keto and amino groups. The blue end shows where the ESP has increased means electron density has decreased and thus the interaction energy with the positive test charge will be more in this region.

Fig. 9 exhibits the UV/visible electronic absorption spectrum of riboflavin. The spectrum shows intense peaks at 245 and 287 nm, while relatively low intensity peaks appear at 375 and 427 nm representing the strength of transitions of the compound. These values deviate from experimental results by about 20–30 nm for all peaks as it is difficult to compute accurate absorption spectrum of riboflavin by most of the available computational methods.

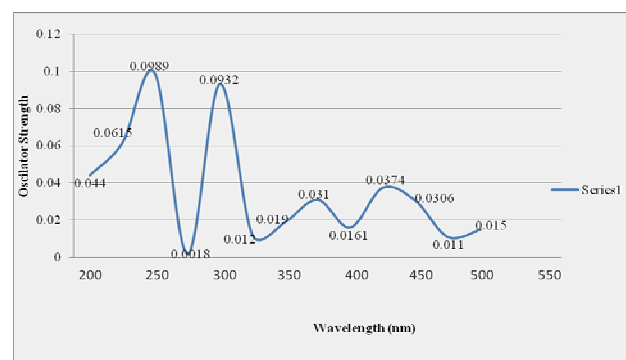


Fig. 9: Electronic absorption spectrum of Riboflavin.

All the results obtained from electron density map, ESP map, and molecular orbital maps represent the active sites with charged groups of the molecule to interact with the receptor.

Such calculations are applicable in determining reaction mechanisms, conducting spectroscopic analysis and in the understanding of the excited-state phenomena as the flavin excited-states are involved in a number of photochemical and photobiological redox reactions.

CONCLUSION

The present work indicates that the best conformation of riboflavin was found to be - 199.2173 kcal/mol which is the minimum potential energy calculated by ArgusLab software. At this point riboflavin will be more active to interact with the receptors. Such types of interactions are significant for drug- receptor interactions.

A useful property of riboflavin and its derivatives is their ability to absorb light. This phenomena is important in finding out electronic transition states (ground-state and excited-state properties) and can be visualized by the

Table 1: Atomic coordinates of riboflavin

S. No.	Atoms	X	Y	Z	R
1	C1	-4.34805239	0.91333229	0.19639601	6
2	C2	-3.69153429	2.20176890	0.51707818	6
3	C3	-2.50633013	2.22594256	1.16190672	6
4	C4	-1.85092472	0.93412851	1.54160775	6
5	C5	-2.42915559	0.22632354	1.19155007	6
6	C6	-3.73132527	0.24268785	0.50788957	6
7	N7	-4.31333506	1.51085998	0.14279162	7
8	C8	-5.62849099	1.52296016	0.45558208	6
9	C9	-6.25346808	0.21977762	0.77635479	6
10	N10	-5.63604978	0.89897145	0.47120217	7
11	C11	-7.54827942	0.20824419	1.46635658	6
12	N12	-6.24319420	-2.6550678	0.71611381	7
13	C13	-7.55935122	2.69079455	1.32382436	6
14	N14	-8.20148035	1.46331456	1.72742401	7
15	O15	-8.24800380	3.91497448	1.45001130	8
16	O16	-8.15789022	1.00254873	1.85462973	8
17	C17	-1.83253602	3.54064643	1.46007227	6
18	C18	-0.64350277	0.89684705	2.43911293	6
19	H19	-4.17780677	3.12704782	0.21617585	1
20	H20	-1.97140812	1.17585410	1.45470772	1
21	H21	-8.00914462	4.26596188	2.39274052	1
22	H22	-7.80895885	1.17608326	281278086	1
23	H23	-0.84737390	3.58636169	0.93980117	1
24	H24	-1.66802945	3.63660324	2.55703101	1
25	H25	-2.44097806	4.41087833	1.12245812	1
26	H26	-0.98946213	0.89303862	3.49798218	1
27	H27	0.01966858	1.77347325	2.2754391	1
28	H28	-0.03743045	0.02170233	2.25930392	1
29	C29	-3.34983298	2.58527408	-0.1003632	6
30	C30	-3.83349155	-.94066195	0.41985172	6
31	C31	-2.89554527	5.06847661	-0.1015642	6
32	C32	-3.27036811	0.50503180	0.35204203	6
33	C33	-3.02440607	6.70520462	1.85490228	6
34	O34	-5.20601022	4.14600909	0.01974519	8
35	O35	-1.53583206	4.78085061	0.31490348	8
36	O36	-4.66537020	6.78280474	0.08357522	8
37	O37	-2.43965384	7.43905070	-0.3898535	8
38	H38	-2.39839401	2.31210610	0.41438038	1
39	H39	-3.16356480	2.63727320	-1.1959803	1
40	H40	-3.78506161	3.90729518	1.52599791	1
41	H41	-2.95791487	5.05245328	-1.2191498	1
42	H42	-3.73232030	7.46031068	2.26072849	1
43	H43	-3.14122503	5.77379237	2.44491768	1
44	H44	-1.99322092	7.06857981	2.02498737	1
45	H45	-5.20232351	4.15757829	-1.0154026	1

Table 2: Bond angles of riboflavin

S. No.	Atoms	Bond Angles	Alternate Bond Angles
1	(C2)-(C1)-(C6)	120.000000	216.488007
2	(C2)-(C1)-(N10)	20.000000	257.053574
3	(C1)-(C2)-(C3)	120.000000	216.488007
4	(C1)-(C2)-(H19)	120.000000	102.928506
5	(C6)-(C1)-(N10)	120.000000	295.980973
6	(C1)-(C6)-(C5)	120.000000	216.488007
7	(C1)-(C6)-(N7)	120.000000	295.980973
8	(C1)-(N10)-(C9)	120.000000	227.550615
9	(C2)-(C3)-(C4)	120.000000	216.488007
10	(C2)-(C3)-(C17)	120.000000	209.804299
11	(C3)-(C2)-(H19)	120.000000	123.034913
12	(C4)-(C3)-(C17)	120.000000	183.094781
13	(C3)-(C4)-(C5)	120.000000	216.488007
14	(C3)-(C4)-(C18)	120.000000	183.094781
15	(C3)-(C17)-(H23)	109.470000	121.420518
16	(C3)-(C17)-(H24)	109.470000	121.420518
17	(C3)-(C17)-(H25)	109.470000	121.420518
18	(C5)-(C4)-(C18)	120.000000	209.804299
19	(C4)-(C5)-(C6)	120.000000	216.488007
20	(C4)-(C5)-(H20)	120.000000	123.034913
21	(C4)-(C18)-(H26)	109.470000	121.420518
22	(C4)-(C18)-(H27)	109.470000	121.420518
23	(C4)-(C18)-(H2)	109.470000	121.420518
24	(C5)-(C6)-(N7)	120.000000	257.053574
25	(C6)-(C5)-(H20)	120.000000	102.928506
26	(C6)-(C7)-(H8)	120.000000	198.144139
27	(C6)-(N7)-(C29)	120.000000	192.403727
28	(C7)-(N8)-(C9)	120.000000	257.053574
29	(N7)-(C8)-(C12)	120.000000	402.764879
30	(N8)-(C7)-(N29)	120.000000	192.403727
31	(C9)-(N8)-(C12)	120.000000	294.480480
32	(C8)-(C9)-(N10)	120.000000	294.480480
33	(C8)-(C9)-(N11)	120.000000	188.442082
34	(C8)-(C12)-(C13)	120.000000	227.506158
35	(C10)-(N9)-(C11)	120.000000	294.480480
36	(N9)-(C11)-(C14)	120.000000	257.053574
37	(C14)-(C11)-(N16)	120.000000	238.736810
38	(C11)-(C14)-(O13)	120.000000	325.928547
39	(N11)-(C16)-(O22)	120.000000	198.144139
40	(C12)-(N13)-(C14)	104.510000	164.040653
41	(C12)-(O13)-(H15)	120.000000	350.783913
42	(N12)-(C13)-(N14)	120.000000	325.928547
43	(N12)-(C13)-(O15)	120.000000	325.928547
44	(N14)-(C13)-(O15)	104.510000	164.040653
45	(C13)-(O15)-(H21)	109.470000	300.071623
46	(N7)-(C29)-(C30)	109.470000	166.826772
47	(N7)-(C29)-(H38)	109.470000	166.826772
48	(N7)-(C29)-(H39)	109.470000	214.211821
49	(C29)-(C30)-(C31)	109.470000	278.259153
50	(C29)-(C30)-(O34)	109.470000	116.984990
51	(C30)-(C29)-(H38)	109.470000	116.984990
52	(C30)-(C29)-(H39)	109.470000	116.984990
53	(C29)-(C30)-(H40)	109.470000	214.211821
54	(C30)-(C31)-(C32)	109.470000	278.259153

S. No.	Atoms	Bond Angles	Alternate Bond Angles
55	(C31)-(C30)-(O34)	109.470000	278.259153
56	(C30)-(C31)-(O35)	109.470000	116.984990
57	(C31)-(C30)-(H40)	109.470000	116.984990
58	(C30)-(C31)-(H41)	109.470000	214.211821
59	(C32)-(C31)-(O35)	109.470000	278.259153
60	(C32)-(C31)-(O36)	109.470000	278.259153
61	(C32)-(C31)-(O37)	109.470000	278.259153
62	(C32)-(C31)-(H41)	109.470000	116.984990
63	(C33)-(C32)-(O36)	109.470000	278.259153
64	(C33)-(C32)-(O37)	109.470000	278.259153
65	(C32)-(C33)-(H42)	109.470000	116.984990
66	(C32)-(C33)-(H43)	109.470000	116.984990
67	(C32)-(C33)-(H44)	109.470000	116.984990
68	(O34)-(C30)-(H40)	109.470000	156.116442
69	(C30)-(C34)-(H45)	109.470000	157.363455
70	(O35)-(C31)-(H41)	109.470000	156.116442
71	(C31)-(O35)-(H46)	109.470000	157.363455
72	(O36)-(C32)-(O37)	109.470000	363.159049
73	(C32)-(O36)-(H47)	109.470000	157.363455
74	(C32)-(O37)-(H47)	109.470000	157.363455
75	(H23)-(C17)-(H24)	109.470000	74.849522
76	(H23)-(C17)-(H25)	109.470000	74.849522
77	(H24)-(C17)-(H25)	109.470000	74.849522
78	(H26)-(C18)-(H27)	109.470000	74.849522
79	(H26)-(C18)-(H28)	109.470000	74.849522
80	(H27)-(C18)-(H28)	109.470000	74.849522
81	(H38)-(C29)-(H39)	109.470000	74.849522
82	(H42)-(C33)-(H43)	109.470000	74.849522
83	(H42)-(C33)-(H44)	109.470000	74.849522
84	(H43)-(C33)-(H44)	109.470000	74.849522

Table 3: Bond lengths of riboflavin

S. No.	Atoms	Bond Lengths
1	C1-----C2	1.458000
2	C1-----C6	1.323387
3	C1-----N10	1.433804
4	C2-----C3	1.323387
5	C3-----C4	1.458000
6	C3-----C17	1.486000
7	C4-----C5	1.323387
8	C4-----C18	1.486000
9	C5-----C6	1.458000
10	C6-----N7	1.433804
11	N7-----C8	1.433804
12	C8-----C9	1.458000
13	C8-----N12	1.301961
14	C9-----N10	1.301961
15	C9-----C11	1.458000
16	C11-----N14	1.433804
17	C12-----O16	1.407689
18	N13-----C13	1.433804
19	C13-----N14	1.433804
20	C13-----O15	1.407689

S. No.	Atoms	Bond Lengths
21	N7---C29	1.461925
22	C29---C30	1.514000
23	C30---C31	1.514000
24	C31---C32	1.514000
25	C32---C33	1.514000
26	C30---O34	1.436155
27	C31---O35	1.436155
28	C32---O36	1.436155
29	C32---O37	1.436155
30	C2---H19	1.084582
31	C5---H20	1.084582
32	O15---H21	1.033746
33	O16---H22	1.033746
34	C17---H23	1.112599
35	C17---H24	1.112599
36	C17---H25	1.112599
37	C18---H26	1.112599
38	C18---H27	1.112599
39	C18---H28	1.112599
40	C29---H38	1.112599
41	C29---H39	1.112599
42	C30---H40	1.112599
43	C31---H41	1.112599
44	C33---H42	1.112599
45	C33---H43	1.112599
46	C33---H44	1.112599
47	O34---H45	1.033746
48	O35---H46	1.033746
49	O36---H47	1.033746
50	O37---H48	1.033746

present study of conformational analysis. The role of these excited-states is of great consequence in understanding of the nature of flavin redox reactions resulting from photochemical processes.

REFERENCES

- Ahmad I, Hussain W and Fareedi AA (1992). Photolysis of cyanocobalamin in aqueous solution. *J. Pharm. Biomed. Anal.*, **10**(1): 9-15.
- Burgstaller P, Hermann T, Huber C, Westhof E and Famulok M (1997). Isoalloxazine derivatives promote photo-cleavage of natural RNAs at G U base pairs embedded within helices. *Nucleic Acids Res.*, **25**: 4018-4027.
- Cramer CJ (2004). Molecular Mechanics. In: Essentials of Computational Chemistry. Theories and Models, 2nd ed., John Wiley and Sons Ltd., England, pp.36-37.
- Crowder GA (1986). Conformational analysis of 3, 3-Dimethylhexane. *Int. J. Rapid. Comm.*, **19**(7): 783-789.
- Dahl MK and Richardson T (1980). Photodegradation of DNA with fluorescent light in the presence of riboflavin and photoprotection by flavin triplet state quenchers. *Biochim. Biophys. Acta*, **610**: 229-234.
- Encinas MV, Bertolotti SG and Previtali CM (2002). The interaction of ground and excited states of lumichrome with aliphatic and aromatic amines in methanol. *Helv. Chim. Acta*, **85**: 1427-1438.
- Fu PP, Cheng SH, Coop L, Xia Q, Culp SJ, Tolleson WH, Wamer WG and Howard PC (2003). Photoreaction, phototoxicity, and photocarcinogenicity of retinoids. *J. Environ. Sci. Health*, **21**(2): 165-197.
- Hirst DM (1990). A Computational Approach to Chemistry. Blackwell Scientific Publications, Oxford. 108-111; 400-403.
- Karelson MM and Zerner MC (1992). Theoretical treatment of solvent effects on electronic spectroscopy. *J. Phys. Chem.*, **96**: 6469-6957.
- Makin HLJ, Jones G, Kaufmann M and Calverly MJ (2010). Analysis of vitamin D, their metabolites and analogues. In: Steroid Analysis, 2nd edition., Springer, UK, pp.967-1096.
- Miura R (2001). Versatility and specificity in flavoenzymes: control mechanisms of flavin reactivity. *Chem. Rec.*, **1**: 183-194
- Mortimer RG (2000). Spectroscopy and Photochemistry. In: Physical Chemistry, 2nd edition., Academic press., USA, pp.774-775.
- Oda A and Takahashi O (2009). Validation of ArgusLab efficiencies for binding free energy calculations. *Chem-Bio Inform. J.*, **9**: 52-61.
- Penzer GR and Radda GK (1970). The chemistry of flavins and flavoproteins. In: Aerobic photochemistry. *Biochim. J.*, **116**: 733-743.
- Powers HJ (2003). Riboflavin and health. *Am. Clin. Nutr.*, **77**: 1353-1360.
- Ridley J and Zerner M (1973). Zindo Semi-empirical Hamiltonian method. Tempelhof Central Airport, Berl. **32**: 111-134.
- Sachiko Y, Keiko Y, Hiroyuki M and Masato S (1999). Three-Dimensional Structure-Function relationship of vitamin D. *Vitamins*, **73**(9): 511-525.
- Sanchez AL, Fernandez S, Verstuyf A, Verlinden L, Gotor V and Ferrero M (2009). Synthesis, conformational analysis and biological evaluation of 19-nor-vitamin D3 analogues with A-ring modifications. *J. Med. Chem.*, **52**(19): 6158- 6162.
- Stewart JJP (1989). Optimization of parameters for semi-empirical methods I-Method. *J. Comp. Chem.*, **10**: 209-220.
- Thompson, M. (2004). ArgusLab 4.0.1. Planaria software LLC, Seattle, W.A.
- Viser AJWG and Muller F (1979). Absorption and fluorescence studies in neutral and cationic isoalloxazines. *Helv. Chim. Acta*, **62**: 593-608.
- Weber G and Teal FWJ (1957). Determination of absolute quantum yield of fluorescent solutions. *Trans Faraday Soc.*, **53**: 646-655.
- Zerner MC (1991). Semiempirical molecular orbital methods. In: Libkowitz, KB and Boyd, DB editors. Reviews in Computational Chemistry, 2nd ed., VCS Publishers Inc., pp.313-366.